ISEIS

Journal of Environmental Informatics 23(2) 58-66 (2014)

Journal of Environmental Informatics

www.iseis.org/jei

Change Detection through Four Techniques Using Multi-Temporal Landsat Thematic Mapper Data: A Case Study on Falavarjan Area, Isfahan, Iran

M. Madanian[1,*], A. Soffianian[1], and A. Hajian[2]

[1]Department of Natural Resources, Isfahan University of Technology, Isfahan 84156-83111, Iran
[2]Faculty of Sciences, Najafabad Branch, Islamic Azad University, Isfahan 8514143131, Iran

Received 18 February 2012; revised 25 April 2013; accepted 15 October 2013; published online 20 June 2014

ABSTRACT. The present study was aimed to assess the applicability of four techniques for detecting changed and unchanged areas in terms of land cover in Falavarjan area, (Isfahan, Iran). The images of the multi-temporal Landsat Thematic Mapper (TM) data acquired on 17 September, 1990 and 13 August, 2010 were used to apply land cover change analysis. The Images were respectively radiometrically and geometrically corrected. The root mean square errors were less than 0.5 pixels for each image. Finally, the image differencing method was used to produce the change image. To separate out the changed and unchanged areas in the difference image, four techniques including Metternicht's method, statistical method, Liu's method and Kapur's method were employed. Among them, the Metternicht's method followed by statistical thresholding technique yielded more accurate binary images.

Keywords: change detection, fuzzy logic, image differencing, Landsat images, thresholding

1. Introduction

Change detection is a process showing the differences of an object or phenomenon at different times (Singh, 1989). Remotely sensed satellite images provides repetitive data such as Thematic Mapper (TM) that are, useful tool for change detection process because of its synoptic view, digital format and cost-effective potential (Nelson et al., 2002; Lu et al., 2004; Chen et al., 2005; Serra et al., 2008). There are different satellite images are used for change detection analysis, of which Landsat data are distinctive as they provide continual and historical images (Wulder et al., 2007).

During recent decades, various change detection techniques have been developed (Coppin et al., 2004). Lunetta (1999) categorized these techniques into two main methods: post-classification and pre-classification. In the first group methods, multi-date satellite images are classified. Then, the classification results are compared and the area of changes determined (Jensen, 2004). However, the latter group methods (including image differencing, image rationing, image regression) locate changes but, do not provide "from-to" matrix (Singh, 1989; Yuan et al., 1999). In this category, image differencing is the most common method for change detection (Jensen and Toll, 1982; Nelson, 1983; Vogelmann, 1988; Singh, 1989; MacLeod and Congalton, 1998; Cheng et al., 2004). Various approaches have been developed for change detection process each of them has its own advantages and disadvantages so that there is no desired and perfect method be applicable to all cases (Bontemps et al., 2008; Concheddaa et al., 2008; Dewan and Yamaguchi, 2009).

Selection of thresholds to distinguish between change and 'no-change' areas is a crucial step for many change detection techniques (Fung and Ledrew, 1988). Two approaches are often applied to define the thresholds (Singh, 1989; Deer, 1995; Yool et al., 1997): (1) Interactive or manual trial-and-error procedure: where an analyst interactively adjusts the thresholds and then evaluates the resulting image until the desired condition is reached; and (2) statistical measure: selection of a suitable standard deviation from a class mean. The disadvantages of the threshold technique are that: (1) resulting differences may be interfered by external effects caused by atmospheric conditions, sun angles, soil moistures and phenological differences in addition to true land-cover change; and (2) threshold is highly subjective and the scene-dependent, making the whole procedure heavily dependent to the skill and familiarity analyst (Lu et al., 2004).

Furthermore, thresholding is accompanied by two types of errors including *commission* and *omission*. Commission and omission errors occur when 'no-change' areas are detected as changed ones and vice versa, respectively (Bruzzone and Fernandez Prieto, 2000).

The present study was aimed to evaluate the efficiency and feasibility of four different techniques for distinguishing of changed and unchanged areas in the difference image as well as to estimate amount of changes that have occurred in

* Corresponding author. Tel.: +98 (0)31 33912841; fax: +98 (0)31 339128 40. *E-mail address:* m.madanian@na.iut.ac.ir (M. Madanian).

ISSN: 1726-2135 print/1684-8799 online
 doi: 10.3808/jei.201400262

Falavarjan area (Isfahan, Iran) during 1990 and 2010.

1.1. Metternicht's Method

According to Zadeh (1965), who proposed the concept of fuzzy logic, a fuzzy set can be mathematically expressed by Equation (1) as follows:

$$A = \{x, \mu_A(x)\};\ x \in X \tag{1}$$

where, X is a space of points (objects), with a generic element of X denoted by x; thus, $X = \{x\}$.

A fuzzy set (class) A in X is characterized by membership (characteristic) function $f_A(x)$ that assigns each point in X a real number in the interval [0,1], with the value of $f_A(x)$ at (x) representing the grade of membership of x in A (Zadeh, 1965).

In a fuzzy set $\mu(x_A) = 0$ shows there is no possibility for the object to belong to the set, while $\mu(x_A) = 1$ indicates the object completely belongs to the set. Values between $\mu(x_A) = 0$ and $\mu(x_A) = 1$ indicate the relative strength of the degree to which the object has properties are typical of the X_A. Therefore, the outcome of a fuzzy classification is a record for every object being analyzed for the degrees to which that object belongs to every single class being considered (Fisher, 2010).

Metternicht (1999) used fuzzy sets and membership functions to improve the change detection results. This method consists of the following steps:

1. In the first step, a fuzzy membership function that fits to the shape of the change image histogram is defined. A bell-shaped membership function proposed by Dombi (1990) is divided into two parts: including a monotonically increasing and a decreasing part. The monotonically increasing function is expressed by Equation (2) as follows:

$$\mu_A(x) = \frac{(1-\nu)^{\lambda-1}(x-a)^{\lambda}}{(1-\nu)^{\lambda-1}(x-a)^{\lambda} + \nu^{\lambda-1}(b-x)^{\lambda}};\ x \in \left[a,b\right] \tag{2}$$

Similarity, the monotonically decreasing function is expressed by Equation (3) as follows:

$$\mu_A(x) = \frac{(1-\nu)^{\lambda-1}(c-x)^{\lambda}}{(1-\nu)^{\lambda-1}(c-x)^{\lambda} + \nu^{\lambda-1}(x-b)^{\lambda}};\ x \in \left[b,c\right] \tag{3}$$

where, λ is sharpness, v denotes the inflection point of the function, a and c are the typical points of the function with a membership degree of zero to the fuzzy set, and b represents the standard point of the variables at the central concept, which is a grade of membership equal to 1 (Dombi, 1990).

2. To reach a form of the membership function fitted to the shape of the change images histogram, two parameters of sharpness and inflection are manipulated. Actually, varying the input parameters, changes the resulting membership function. Therefore, if the resulting membership functions fit the shape of a change image, discrimination of 'change' and 'no-change' areas will be performed with a high accuracy.

3. As Zadeh (1984) states, fuzzy logic technique uses graded or qualified statements rather than the strictly true or false items. In fuzzy logic theory, fuzzy quantifiers such as 'likely' and 'usually' are treated as fuzzy numbers representing, imprecisely, the absolute or relative count of elements in a fuzzy set (Zadeh, 1984). Linguistic constructs were used to describe changes where, possibility of change, ranging of 0 to 1, is expressed using some linguistics terms.

4. Finally, the change image is mapped in a gray scale ranging from white to black. In this way, pixels with an absolute certainty of 'no-change' are represented by white, whereas changed areas are represented by black where changes are occurred with absolute certainty (Metternicht, 1999).

1.2. Statistical Thresholding Method

In this method, change and unchanged areas were distinguished according to the histogram of the values. In the histogram, unchanged pixels are distributed at or around the mean and changed pixels are located at two tails of histogram. Various levels of threshold can be applied to the lower and higher tail to determine the optimal threshold that subsequently resulted in the highest accuracy (Fung and Le Drew, 1988).

1.3. Liu's Method

Liu et al. (2006) selected the optimal threshold t_l based on a fuzzy entropy measurement. They considered both inter-class distinctness and intra-class variation criteria. The objective of thresholding is grouping the difference image into two classes, namely, ω_c and ω_u corresponding to 'changed' and 'unchanged' classes. Let the number of pixels in the image with grey level i be f_i. Then the total number of pixels in the difference image with size of $p \times q$ is expressed as $\sum_{i=0}^{L-1} f_i (= p \times q)$. Substituting the proper variables will define the probability of occurrence of grey level i (denoted as p_i) *as* Equation (4) (Patra et al., 2011):

$$p_i = \frac{f_i}{p \times q} \tag{4}$$

As defined by Huang and Wang (1995), the fuzzy membership value for a pixel with grey value i in D is given by Equation (5):

$$\mu_D(i) = \begin{cases} \dfrac{1}{1+\left|i-\mu_{\omega_u}\right|/C} & \text{if } i \le t \\ \dfrac{1}{1+\left|i-\mu_{\omega_c}\right|/C} & \phantom{\text{if }} i > t \end{cases} \tag{5}$$

where C is a constant which follows the $0.5 \le \mu_D(i) \le 1$ condition.

The fuzzy entropies of unchanged (ω_u) and changed (ω_c) classes, denoted by $H\omega_u(t)$ and $H\omega_c(t)$, respectively, are then computed by Equations (6) and (7) as follows:

$$H_{\omega_u}(t) = -\sum_{i=0}^{t} \frac{p_i}{\mu_D(i)P_{\omega_u}} \log \frac{p_i}{\mu_D(i)P_{\omega_u}} \tag{6}$$

$$H_{\omega_c}(t) = -\sum_{i=t+1}^{L-1} \frac{p_i}{\mu_D(i)P_{\omega_c}} \log \frac{p_i}{\mu_D(i)P_{\omega_c}} \tag{7}$$

where $P_{\omega_u} = \sum_{i=0}^{t} \frac{p_i}{\mu_D(i)}$ and $P_{\omega_c} = \sum_{i=t+1}^{L-1} \frac{p_i}{\mu_D(i)}$.

Equations (6) and (7) define the entropy of distribution of the ratio of the grey-scale histogram and fuzzy membership of unchanged and changed pixels for threshold t .The optimal threshold t_1 is obtained by maximizing $\{H\omega_u(t) + H\omega_c(t)\}$ over t. The condition is expressed in Equation (8) as follows:

$$t_1 = Arg \max_{t \in z} \left\{ H_{\omega_u}(t) + H_{\omega_c}(t) \right\} \tag{8}$$

1.4. Kapur's Method

Kapur et al. (1985) proposed that the optimal threshold can be determined based on the concept of entropy (Shannon, 1948). Two probability distributions, one for (ω_u) and the other for (ω_c) are derived from the original grey level distribution of the difference image D by assuming a threshold value t as follows:

$$\omega_u : \frac{p_0}{P_{\omega_u}}, \frac{p_1}{P_{\omega_u}}, ..., \frac{p_t}{P_{\omega_u}}, \text{ and } \omega_c : \frac{p_{t+1}}{P_{\omega_c}}, \frac{p_{t+2}}{P_{\omega_c}}, ..., \frac{p_{L-1}}{P_{\omega_c}}$$

where $P_{\omega_u} = \sum_{i=0}^{t} p_i$ and $P_{\omega_c} = 1 - P_{\omega_u}$.

The entropies of the unchanged (ω_u) and changed (ω_c) classes are then determined using Equations (9) and (10) as follows:

$$H_{\omega_u}(t) = -\sum_{i=0}^{t} \frac{p_i}{P_{\omega_u}} \log_2 \left(\frac{p_i}{P_{\omega_u}}\right) \tag{9}$$

$$H_{\omega_c}(t) = -\sum_{i=t+1}^{L-1} \frac{p_i}{P_{\omega_c}} \log_2 \left(\frac{p_i}{P_{\omega_c}}\right) \tag{10}$$

The optimal threshold t_1 is determined through maximizing the total entropy $\{H\omega_u(t) + H\omega_c(t)\}$ using the rule expressed by Equation (11) as follows:

$$t_1 = Arg \max_{t \in z} \left\{ H_{\omega_u}(t) + H_{\omega_c}(t) \right\} \tag{11}$$

2. Study Area and Data

The study area is Falavarjan area located in western part of Isfahan (Iran). It covers about 17550.6 ha and located in 32°29' ~ 32°37' N and 51°20' ~ 51°35' E. Falavarjan city, located in the center of the study area, is on the bank of Zayandehrud River (Figure 1). Zayandehrud River emanates from Zardkuh Mountain and flows in eastern Falavarjan. The climate is hot and dry with an average temperature of about 16.4 °C and average annual rainfall of 162 mm/year.

The study area includes agricultural fields, Zayandehrud River, Zob Ahan Highway, bare lands, rocky outcrops, and urban areas. If water and land are suitably managed, this area has a good potential for agriculture expansion.

In this study, two Landsat-5 Thematic Mapper (TM) images acquired on September 17, 1990 and August 13, 2010 (path 164, row 37) were utilized to detect land cover changes over a period of 20 years, respectively.

3. Methods

3.1. Image Pre-Processing

Numerous factors such as different imaging dates, different solar altitudes, and different meteorological conditions can affect radiometric conditions. Therefore, it is essential to perform radiometric correction before change detection (Paolini et al., 2006). Radiometric correction modifies digital number values to reduce or remove sensor or atmospheric noise (Gong et al., 2008).

3.1.1. Absolute Radiometric Correction

Absolute radiometric correction has two steps. First, the digital number (DN) of the sensor measurements are converted to spectral radiance measured by satellite sensors using Equation (12):

$$L_{sat} = DN * Gain + Offset \tag{12}$$

Here, L_{sat} is the spectral radiance detected by a satellite sensor; DN is the digital number of the sensor measurement, and Gain and Offset are sensor specific calibration parameters determined prior to sensor launch. While these parameters are usually assumed to be stable, they can change due to long-time service or accidents (Schowengerdt, 1997).

The next step is to transfer the sensor detected radiance into ground surface reflectance using Equation (13) (Lillesand

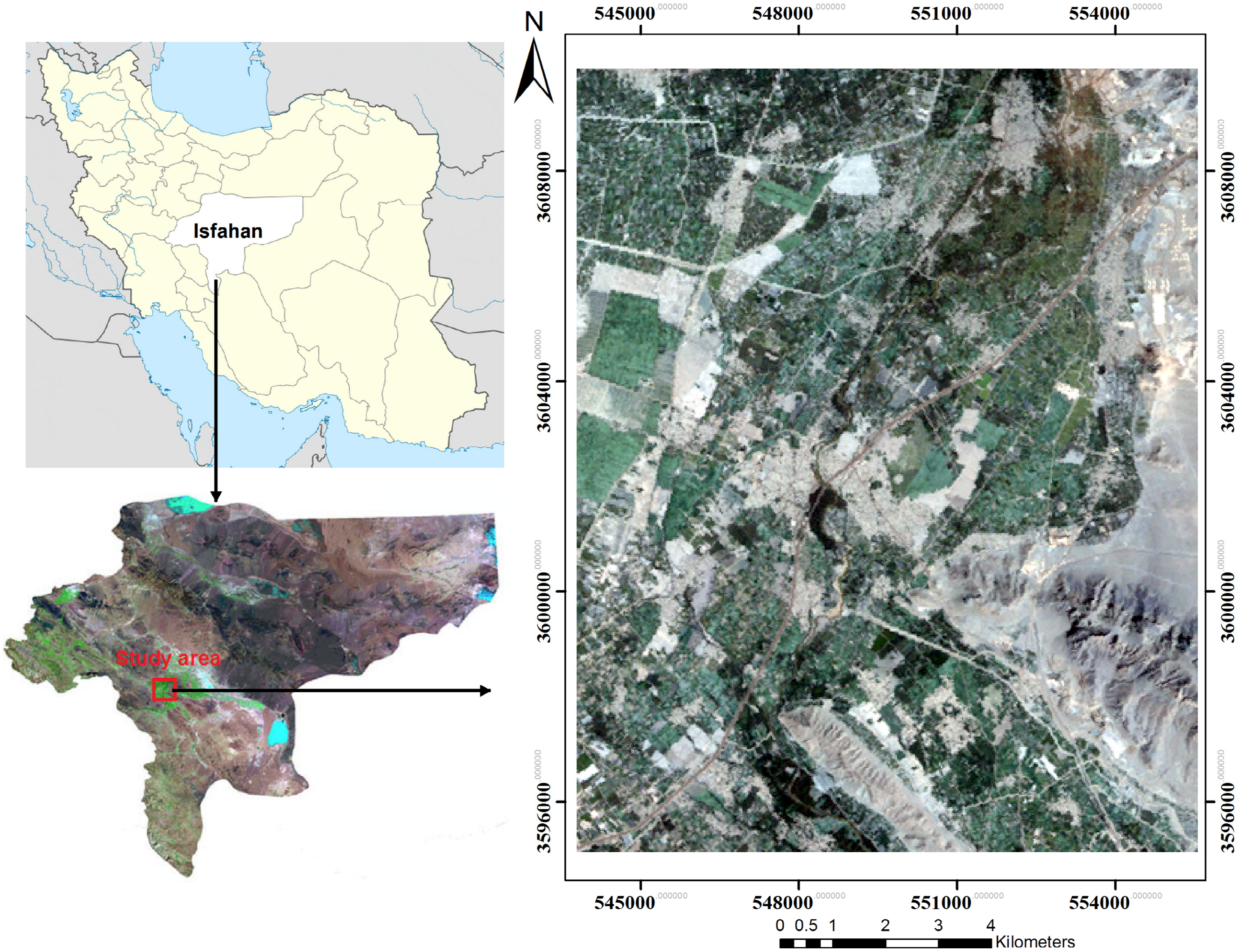

Figure 1. Study area: Landsat TM image of Falavarjan area, collected on 17 September 1990 (right) in the west of Isfahan city (below left) and Iran (above left).

and Kiefer, 1994):

$$\rho_{surface} = \frac{(L_{sat} - L_{path})\pi}{E_{\tau}} \tag{13}$$

where $\rho_{surface}$ is the ground surface reflectance of the target. L_{path} is the path radiance, E is the irradiance on the ground target, and τ is the transmission of the atmosphere (Lillesand and Kiefer, 1994).

3.1.2. Geometric Correction

Accurate geometric correction of multi-temporal images is necessary for any change detection technique since inaccurate registration leads to an overestimation of real change (Stow, 1999; Verbyla and Boles, 2000). Most change detection methods are affected by accuracy of geometric correction (Dai et al., 1996). The root mean square error (RMSe), a crucial factor in assessing the accuracy of registration, should not exceed 0.5 pixels (Lunetta and Elvidge, 1998; Jensen, 2005).

In this paper, digital images were georeferenced to the Universal Transverse Mercator (UTM) projection (zone 39) with a spatial resolution of 28.5 m using approximately 40 ground control points (GCPs) per image. Ground control points were extracted from digitized map with the scale of 1:50000 for the earlier image. For the later image, using a Global Positioning System (GPS) device, 40 ground control points were selected in the field. These control points covered the study area with the uniform distribution. Rectification was carried out using a first order polynomial model and the nearest neighborhood resampling method. RMSE were less than 0.5 pixels for each image, which is acceptable.

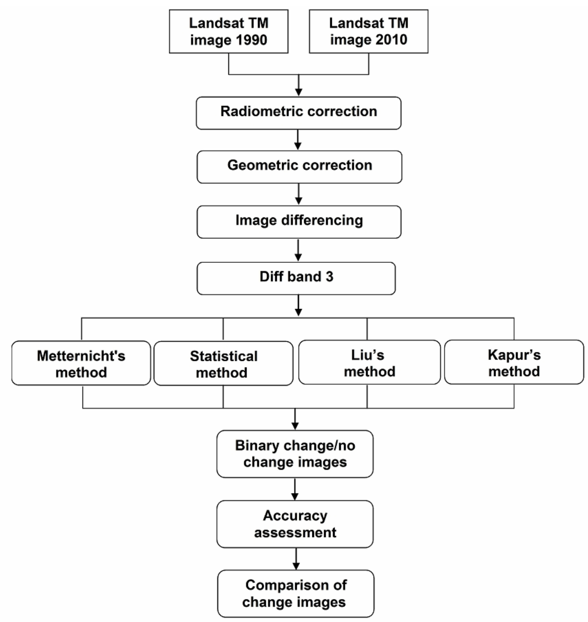

Figure 2. General sequence of change detection process.

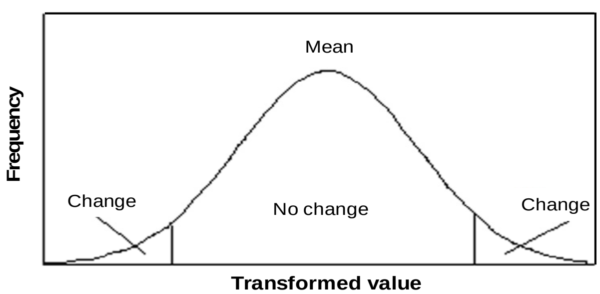

Figure 3. Threshold application.

3.2. Change Detection Process

Various techniques are used to identify binary change and non-change information (Lu et al., 2004). This study employed image differencing approach to produce change images. Then, the change image was used as an input of four methods including Metternicht's method, statistical method, Liu's method and Kapur's method to discriminate changed and unchanged areas. The process of change detection is depicted in Figure 2.

3.2.1. Image Differencing

Image differencing method produces a change image by subtracting two or more datasets. Digital numbers in the resultant difference image are often considered to be normally distributed so that pixels with small change are observed around the mean. Pixels with substantive changes are distributed in the tails of histogram (Singh, 1989) (Figure 3). The main advantages of this technique are its simplicity and ease of interpretation of the change images. However, selecting the best threshold that identifies the change from non-change areas is a crucial step (Lu et al., 2005). In this study, all reflective bands, excluding the thermal band, were used in the change detection. The change image was produced by subtracting the 1990 image band 3 from the 2010 image band 3 pixel-by-pixel.

3.3. Accuracy Assessment

To assess the accuracy of change images created by four techniques, topographic maps on the scale of 1:25000 and 1:50000 related to 1990 and 2010 were used, respectively. Moreover, field survey records were applied to improve the results of accuracy assessment. The process of accuracy assessment was based on a stratified random sampling approach so that 150 Sample points were selected on the topographic maps. An area of 3 × 3 pixels was interpreted for each sample point. The change images were assessed against sample of reference points using an error matrix made for each image. Comparison of outcomes of each method was based on Kappa coefficient, overall accuracy, commission and omission errors derived from error matrix table. The error matrix is the most common technique for accuracy assessments (Lu et al., 2004).

4. Results and Discussion

For change detection analysis, it is critical to choose appropriate image bands (Lu et al., 2005). In this study, bands 3 was chosen for two reasons: (1) the dominant land cover in the study site is vegetative cover and band 3 has the good potential to indicate changes that have occurred in this class (Jenson and Toll, 1982; Hame, 1986; Pilon et al., 1988; Fung, 1990; Ridd and Liu, 1998; Lu et al., 2004). (2) Digital numbers of the change image created by bands 3 were normally distributed.

The error matrix was used to analyze the accuracy of the classified change images using different methods. Ground true data, color composite imageries and topographic maps were used to generate the error matrix. To estimate the overall accuracy, the total correct pixels were divided by the total number of pixels. Table 1 shows Kappa and overall accuracy obtained by the four methods. Among them, the Mettrnicht's method followed by statistical technique is found to be the most accurate ones. Accuracy of the outcome of Mettrnicht's method is significantly dependent on the two parameters, including sharpness and inflection which obtained through trial and error. Table 2 shows the optimized values for these two parameters. Appling these values formed the optimized membership functions that fitted to the shape of the change image histogram. The more two histograms fit, the more accurate results achieve. Figure 4 depicts the optimized membership functions for change images. In this way, mean is considered as a standard point that represents pixels of 'no-change' with a membership degree of 1. Typical points are tail

Table 1. Change Detection Results Obtained by Applying Different Methods

Overall error	No-change		Change		Overall accuracy (%)	Kappa (%)	Method
	OE**	CE*	OE**	CE*			
0.13	0.07	0.12	0.24	0.15	86.8	70.2	Metternicht
0.13	0.08	0.13	0.25	0.16	86.2	69	Statistical
0.19	0.24	0.06	0.09	0.33	81.1	61.6	Liu
0.18	0.21	0.07	0.10	0.31	82.3	63.6	Kapur

CE*: Commission error.
OE**: Omission error.

Table 2. Values for Parameters of Membership Functions of the Change Image

Change image	Sharpness (λ)		Inflection (ν)		Standard point	Typical points
	MI*	MD**	MI*	MD**		
Diff3	2.4	2.6	0.9	0.95	0.24	-10.2 and 13.3

* MI: Monotonically increasing part of the function.
** MD: Monotonically decreasing part of the function.

Table 3. Results of Area Estimation Using Mettrnicht's Method

Code	Fuzzy linguistic terms	Degree of membership	Number of pixels	Area (ha)	Percentage
1	No changes	0.81 to 1.00	123881	9712.3	55.3
2	Very unlikely changes	0.61 to 0.80	27671	2169.4	12.4
3	Unlikely changes	0.51 to 0.60	12714	996.8	5.7
4	Neither nor	0.41 to 0.50	10805	847.1	4.8
5	Likely changes	0.31 to 0.40	10446	818.9	4.7
6	Very likely changes	0.21 to 0.30	12051	944.8	5.4
7	Extremely likely changes	0.11 to 0.20	12412	973.1	5.5
8	Changes	0.00 to 0.10	13880	1088.2	6.2

* Area (ha) = 0.0784 ha × number of pixels, as the TM image has a 28.5 m resolution.

values of the histogram that signify change pixels. The membership degree of 0 is assigned to these change pixels. The resultant fuzzy image had 8 classes which visualized in a gray scale (Figure 5). In such a way, a spectrum of white to show pixels has never changed to black depicting areas that have definitely undergone changes. Table 3 represents results of area estimation obtained by Mettrnicht's method.

To derive changed and unchanged parts, the fuzzy image was converted to the binary change image by applying defuzzification. Therefore, different thresholds including 0.4, 0.5 and 0.6 were tested to separate changed and unchanged areas. The images obtained from these thresholds were compared against the reference data. Results showed that 0.5 was the most accurate one. In this method, the proportions of the changed and unchanged area were 59594 and 164266 pixels, respectively. The kappa coefficient and an overall accuracy of the resultant image were 70.2 and 86.8%, respectively. Figure 6(a) represents the binary fuzzy change image.

Another method used here to detect changed and unchanged areas was based on a statistical thresholding technique. In this paper, Threshold levels, ranging from 0.8 to 3.0 standard deviations from the mean, were tested on the change image to determine the most suitable threshold values. Then, the change image was reclassified into two classes. The value '0' was assigned for 'no-change' areas and '1' for change

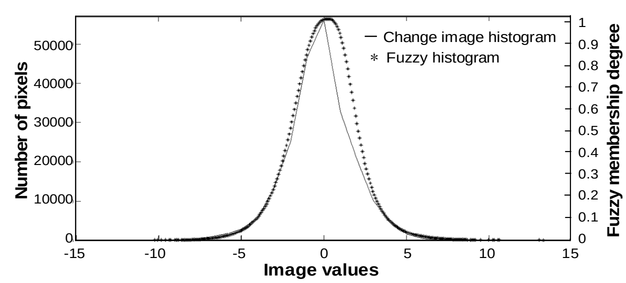

Figure 4. Optimized membership function for the Falavarjan change images, where μ is the membership degree to set of 'no change'.

areas. Consequently, 1σ was identified as the most accurate one among others with the kappa coefficient and an overall accuracy of 69 and 86.2%, respectively. In practice, the thresholds are often specified by one standard deviation from the mean or with some modification (Singh, 1989; Ridd and Liu, 1998).This procedure resulted in an image containing 62104 changed and 161756 unchanged pixels (Figure 6(b)).

Liu's method and Kapur's method were the other techniques which used. In this investigation, the overall accuracies of images produced by Liu's and Kapur's methods were 81.1 and 82.3%, respectively. Table 4 shows that thresholds which detected by the two methods are close to

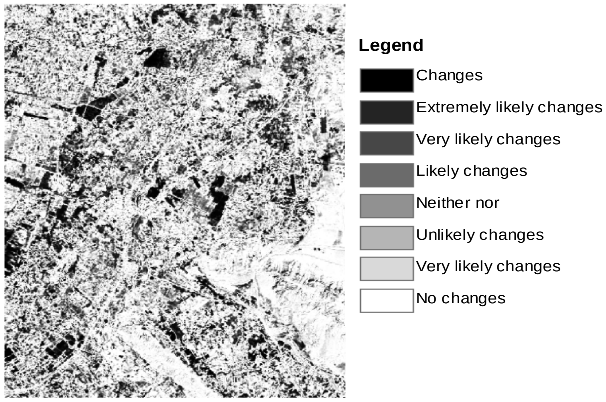

Figure 5. The resultant image obtained by Mettrnicht's method.

each other. As a result of applying Liu's method, 108964 changed and 114896 unchanged pixels were identified. The image created by Kapur's method contains 103468 changed and 120392 unchanged pixels (see Figure 6(c) and 6(d)). Kapur's method is one of the best techniques to thresholding (Radke et al., 2005). In Kapur's method the optimal threshold is identified by maximizing the entropy of the changed and unchanged classes. It changes the histogram of the difference image so as to have a more or less equal distribution for changed and unchanged classes (Patra et al., 2011). Kapur's method is the classical thresholding technique to discriminate changed and unchanged regions based on the entropy concept while Liu's method is based on fuzzy entropy. Liu's method considers not only inter-class distinctness, but also intra-class variation which may help select better thresholds. Basically, the entropy defined by Liu contains Kapur's entropy (Kapur et al., 1985) in itself and introduces a fuzzy concept to manage the natural fuzziness of images. Among the procedures applied here, the most time consuming technique was Liu's method. The threshold and time of each method are shown in Table 4.

By analyzing the results shown in Table 1, it is noticed that the highest overall error assigns to Liu's method. The overall accuracies and overall errors of Mettrnicht's method and statistical technique are close to each other. This table represents two kinds of errors obtained by applying each technique. Omission error occurs when an area is omitted from the correct category. Commission error occurs when an area is placed in the wrong category.

According to the Metternicht's method as the most accurate approach, 73.3% of the study area remained unchanged and 26.6% of the area has undergone changes. The unchanged class mainly covers eastern and southern parts of the study area, which rocky outcrops where no changes had occurred during 1990 ~ 2010. Zob Ahan Highway is another part of Falavarjan area that has been remained unchanged. The changed area includes bare lands and agricultural areas that have been replaced by each other. These changes are also observable around the urban area which has expanded since 1990. The number of pixels and area of changed and unchanged parts obtained by each method are represented in Table 5.

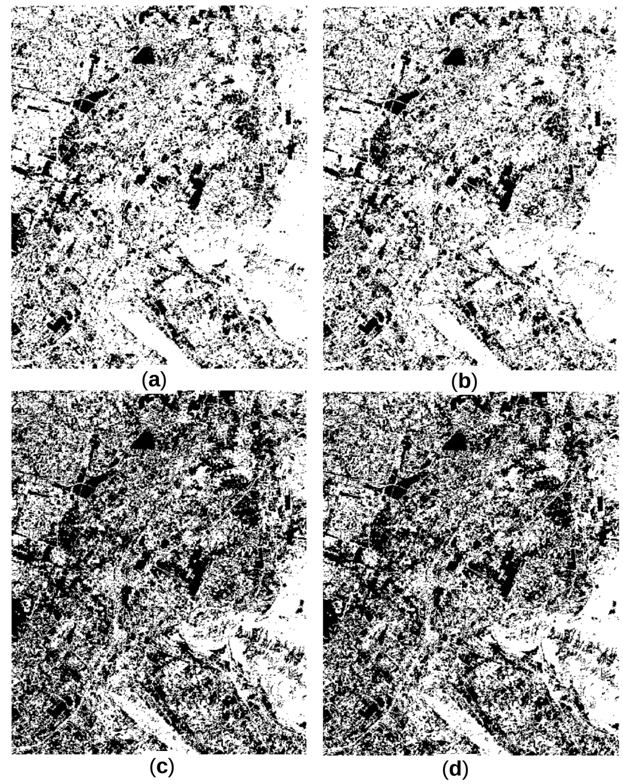

Figure 6. The resultant binary change images created for Falavarjan area using (a) Mettrnicht's method, (b) Statistical method, (c) Liu's method and (d) Kapur's method. Black and white shows changed and unchanged pixels, respectively.

Table 4. Optimal Threshold, Time and Iteration for Different Techniques

Time (s)	threshold	Methods
390	-	Metternicht
-	2	Statistical
706	1.1	Liu
359	1.2	Kapur

Table 5. The Number of the Change/No-Changed Pixels and the Area of Each Class Detected by Four Methods

Method	Change		No-change	
	Pixels	Area (ha)	Pixels	Area (ha)
Metternicht	59594	4672.2	164266	12878.4
Statistical	62104	4868.9	161756	12681.7
Liu	108964	8542.8	114896	9007.8
Kapur	103468	81119	120392	9438.7

As a final comparison, although the overall accuracies of Metternicht's method and statistical technique are close to each other, fuzzy change model can identify a continuum value of changes. As the fuzzy logic is based on inaccuracy modeling with membership function, not only does it improve the accuracy of the results to distinguish changed and unchanged areas, but also it is able to help the interpreter know to what extent the degree of 'change' and 'no-change' is for the area. The application of the fuzzy set theory to knowledge-based systems offers advantages in terms of: (1) representation and processing of uncertain data in the form of fuzzy sets (*e.g.* a moderately saline class), and (2) representation of vague knowledge in the form of linguistic rules with imprecise terms defined as fuzzy sets. Therefore, fuzzy logic can provide a powerful approach for classifying and monitoring environmental conditions related to salinity, and for describing the nature and severity of changes occurring over time (Fisher, 2010). Each pixel has been labeled with code '0' ('no-change' areas) or '1' (change areas) in both techniques (Figure 7). To make the interpretation of change images produced by two methods easier, the membership degree of the pixel to the set of 'change' is represented so that the higher the membership degree, the more the areas have changed.

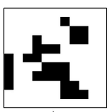

(a)

Col/row	0	1	2	3	4	5	6	7	8	9
0	0	0	0	0	0	0	0	0	0	0
1	0	0	0	0	0	0	1	0	0	0
2	0	0	0	0	0	0	0	1	1	0
3	0	0	0	1	0	0	0	1	1	0
4	0	0	0	1	1	1	0	0	0	0
5	1	0	1	1	0	0	0	0	0	0
6	1	0	0	0	1	1	1	0	0	0
7	1	0	0	1	1	1	1	0	0	0
8	1	0	0	0	0	0	1	1	0	0
9	0	0	0	0	0	0	1	1	1	0

(b)

Col/row	0	1	2	3	4	5	6	7	8	9
0	0.17	0.01	0.09	0.01	0.01	0.01	0.03	0.01	0.22	0.09
1	0.17	0.03	0.27	0.23	0.07	0.07	0.66	0.51	0.44	0.02
2	0.30	0.07	0.02	0.21	0.05	0.05	0.34	0.75	0.71	0.04
3	0.23	0.01	0.23	0.64	0.19	0.19	0.27	0.83	0.63	0.05
4	0.06	0.01	0.47	0.66	0.80	0.80	0.23	0.23	0.54	0.11
5	0.53	0.09	0.64	0.68	0.23	0.23	0.37	0.11	0.23	0.09
6	0.47	0.30	0.01	0.41	0.73	0.73	0.68	0.01	0.04	0.34
7	0.86	0.36	0.03	0.58	0.78	0.78	0.68	0.27	0.04	0.01
8	0.58	0.17	0.11	0.02	0.01	0.01	0.73	0.78	0.27	0.17
9	0.24	0.01	0.05	0.03	0.17	0.17	0.86	0.96	0.88	0.05

Figure 7. Example of selecting change image matrix obtained by (a) statistical (b) Mettrnicht's method. For both of the figures, the code '0' was assigned for 'no change' areas and the code '1' for changed areas. Note that here μ is the degree of membership to set of 'change'.

5. Conclusions

Various approaches have been developed for change detection process each of them has its own advantages and disadvantages. In this research, image differencing approach was applied to produce change image because it is simple and straightforward. Image differencing is one of the most common change detection methods. In this research, to separate changed and unchanged areas, four methods were applied. Among the techniques applied in this paper, Metternicht's method produced the best results. On the other hand, statistical thresholding technique yielded the accurate results followed by Kapur's technique. Liu's method had the least accuracy.

As a final remark, fuzzy change model made the interpretation of the results easier because 'linguistic' labels are simpler for the interpreter as well as non-expert users. This approach has several advantages compared with the conventional change detection methods that can be summarized as follows:

(i) Change between different dates cannot always be grouped into separate classes; however, there may exist a continuum of change.

(ii) In this procedure, inaccuracies (*commission* and *omission* errors) caused by selecting thresholds were removed.

(iii) This method helps decision-makers to identify areas which have changed as well as to estimate the amount of changes over time.

Acknowledgements. This research has been supported by the Isfahan University of Technology (IUT).

References

Bontemps, S., Bogaert, P., Titeux, N., and Defourny, P. (2008). An object-based change detection method accounting for temporal dependences in time series with medium to coarse spatial resolution. *Remote Sens. Environ.,* 112 (6), 3181-3191. http://dx.doi.org/10.1016/j.rse.2008.03.013

Bruzzone, L., and Fernandez Prieto, D. (2000). A minimum-cost thresholding technique for unsupervised change detection. *Int. J. Remote Sens.,* 21 (18), 3539-3544. http://dx.doi.org/10.1080/014311600750037552

Chen, X., Vierling, L., and Deering, D. (2005). A simple and effective radiometric correction method to improve landscape change detection across sensors and across time. *Remote Sens. Environ.,* 98 (1), 63-79. http://dx.doi.org/10.1016/j.rse.2005.05.021

Cheng, K.S., Wei, C., and Chang, S.C. (2004). Locating landslides using multi-temporal satellite images. *Adv. Space Res.,* 33 (3), 296-301. http://dx.doi.org/10.1016/S0273-1177(03)00471-X

Concheddaa, G., Durieuxb, L., and Mayauxa, P. (2008). An object-based method for mapping and change analysis in mangrove ecosystems. *ISPRS J. Photogramm. Remote Sens.,* 63 (5), 578-589. http://dx.doi.org/10.1016/j.isprsjprs.2008.04.002

Coppin, P., Jonckheere, I., Nackaerts, K., Muys, B., and Lambin, E. (2004). Review article digital change detection methods in ecosystem monitoring: a review. *Int. J. Remote Sens.,* 25 (9), 1565-1596. http://dx.doi.org/10.1080/0143116031000101675

Dai, X., Khorram, S., and Cheshire, H. (1996). Automated image registration for change detection from Thematic Mapper imagery, Proc. of the IEEE International Geoscience and Remote Sensing Symposium, (IGARSS'96), Lincoln, NE, 1601-1603.

Deer, P.J. (1995). Digital change detection techniques: civilian and military applications, International Symposium on Spectral Sensing Research 1995 Report (Greenbelt, MD: Goddard Space Flight Center), http://ltpwww.gsfc.nasa.gov/ISSSR-95/digitalc.htm.

Dewan, A.M., and Yamaguchi, Y. (2009). Land use and land cover change in Greater Dhaka, Bangladesh: using remote sensing to promote sustainable urbanization. *Appl. Geogr.,* 29 (3), 390-401. http://dx.doi.org/10.1016/j.apgeog.2008.12.005

Dombi, J. (1990). Membership function as an evaluation. *Fuzzy Sets Syst.,* 35 (1), 1-21. http://dx.doi.org/10.1016/0165-0114(90)90014-W

Fisher, P.F. (2010). Remote sensing of land cover classes as type 2 fuzzy sets. *Remote Sens. Environ.,* 114 (2), 309-321. http://dx.doi.org/10.1016/j.rse.2009.09.004

Fung, T. (1990). An assessment of TM imagery for land cover change detection. *IEEE Trans. Geosci. Remote Sens.,* 28 (4), 681-684. http://dx.doi.org/10.1109/TGRS.1990.572980

Fung, T., and Ledrew, E. (1988). The determination of optimal threshold levels for change detection using various accuracy indic

-es. *Photogramm. Eng. Remote Sens.,* 54 (10), 1449-1454.

Gong, J., Sui, H., Ma, G., and Zhou, Q. (2008). A review of multi -temporal remote sensing data change detection algorithms. The International Archives of the Photogrammetry, Remote Sensing and Spatial Information Sciences, 37, Part B7. Beijing.

Hame, T.H. (1986). Satellite image aided change detection. In: Remote sensing-aided forest inventory. Research Notes. Depart -ment of Forest Mensuration and Management, University of Hel -sinki, Helsinki, Finland.

Huang, L.K., and Wang, M.J.J. (1995). Image thresholding by mini -mizing the measures of fuzziness. *Pattern Recogn.,* 28(1), 41-51. http://dx.doi.org/10.1016/0031-3203(94)E0043-K

Jensen, J.R. (2004). Digital Change Detection. Introductory digital image processing: A remote sensing perspective. Prentice-Hall, New Jersey.

Jensen, J.R. (2005). Introductory Digital Image Processing: A Remo -te Sensing Normalized. Prentice-Hall, New Jersey.

Jensen, J.R., and Toll, D.L. (1982). Detecting residential land use development at the urban fringe. Photogramm. *Eng. Remote Sens.,* 48 (4), 629-643.

Kapur, J.N., Sahoo, P.K., and Wong, A.K.C. (1985). A new method for gray-level picture thresholding using the entropy of the histo -gram. *Comput Vision Graph.,* 29(3), 273-285. http://dx.doi.org/ 10.1016/0734-189X(85)90125-2

Lillesand, T.M., and Kiefer, R.W. (1994). Remote Sensing and Image Interpretation. John Wiley & Sons.

Liu, D., Jiang, Z., and Feng, H., (2006). A novel fuzzy classification entropy approach to image thresholding. *Pattern Recogn Lett.,* 27, 1968-1975. http://dx.doi.org/10.1016/j.patrec.2006.05.006

Lu, D., Mausel, P., Batistella, M., and Moran, E. (2005). Land-cover binary change detection methods for use in the moist tropical region of the Amazon: a comparative study. *Int. J. Remote Sens.,* 26 (1), 101-114. http://dx.doi.org/10.1080/014311604100017 0748

Lu, D., Mausel, P., Brondizio, E., and Moran, E. (2004). Change detection techniques. *Int. J. Remote Sens.,* 25 (12), 2365-2401. http://dx.doi.org/10.1080/0143116031000139863

Lunetta, R.S. (1999). Applications, Project Formulation and Analyti -cal Approach. In Remote sensing change detection: Environmen -tal monitoring methods and applications. Taylor & Francis, Lon -don.

Lunetta, R.S., and Elvidge, C.D. (1998). Remote Sensing Change Detection. Michigan: Ann Arbor Press.

Macleod, R.D., and Congalton, R.G. (1998). A quantitative com-parison of change-detection algorithms for monitoring eelgrass from remotely sensed data. Photogramm. *Eng. Remote Sens.,* 64, 207-216.

Metternicht, G. (1999). Change detection assessment using fuzzy sets and remotely sensed data: an application of topographic map revi -sion. *ISPRS J. Photogramm. Remote Sens.,* 54(4), 221-233. http:// dx.doi.org/10.1016/S0924-2716(99)00023-4

Nelson, R.F. (1983). Detecting forest canopy change due to insect activity using Landsat MSS. Photogramm. *Eng. Remote Sens.,* 49 (9), 1303-1314.

Nelson, S.A.C., Sorrano, P.A., and Qi, J. (2002). Land cover change in the Upper Barataria Basin Estuary, Louisiana, from 1972–1992: increases in wetland area. *J. Environ. Manage.,* 29 (5), 716-727. http://dx.doi.org/10.1007/s00267-001-0060-9

Paolini, L., Grings, F., Sobrino, J.A., Muñoz, J.C.J., and Karszen-baum, H. (2006). Radiometric correction effects in Landsat multi-date/multi-sensor change detection studies. *Int. J. Remote Sens.,* 27 (4), 685-704. http://dx.doi.org/10.1080/01431160 500183057

Patra, S., Ghosh, S., and Ghosh, A. (2011). Histogram thresholding for unsupervised change detection of remote sensing images, *Int. J. Remote Sens.*, 32 (21), 6071-6089. http://dx.doi.org/10.1080/01431 161.2010.507793

Pilon, P.G., Howarth, P.J., Bullock, R.A., and Adeniyi, P.O. (1988). An enhanced classification approach to change detection in semi -arid environments. Photogramm. *Eng. Remote Sens.,* 54 (12), 1709-1716.

Radke, R.J., Andra, S., Al-Kofahi, O., and Roysam , B. (2005). Image change detection algorithms: A systematic survey. *IEEE T Image Process.,* 14(3). 294-307. http://dx.doi.org/10.1109/TIP.2004.838 698

Ridd, M.K., and Liu, J. (1998). A comparison of four algorithms for change detection in an urban environment. *Remote Sens. Environ.,* 63(2), 95-100. http://dx.doi.org/10.1016/S0034-4257(97)00112-0

Schowengerdt, R.A. (1997). Remote Sensing Models and Methods for Image Processing. 2nd edition. San Diego, CA: Academic Pre -ss Ltd.

Serra, P., Pons, X., and Sauri, D. (2008). Land-cover and land-use change in a Mediterranean landscape: a spatial analysis of driving forces integrating biophysical and human factors. *Appl. Geogr.,* 28 (3), 189-209. http://dx.doi.org/10.1016/j.apgeog.2008.02.001

Shannon, C.E. (1948). A mathematical theory of communication. *Bell Syst Tech J.,* 27, 379-423. http://dx.doi.org/10.1002/j.1538-7305. 1948. tb0 1338.x

Singh, A. (1989). Digital change detection techniques using remotely sensed data. *Int. J. Remote Sens.,* 10 (6), 989-1003. http://dx.doi. org/10.1080/01431168908903939

Stow, D.A. (1999). Reducing misregistration effects for pixel-level analysis of land-cover change. *Int. J. Remote Sens.,* 20(12), 2477-2483. http://dx.doi.org/10.1080/014311699212137

Verbyla, D.L., and Boles, S.H. (2000). Bias in land cover change estimates due to misregistration. *Int. J. Remote Sens.,* 21 (18), 3553-3560. http://dx.doi.org/10.1080/014311600750037570

Vogelmann, J.E. (1988). Detection of forest change in the Green Mountains of Vermont using multi spectral scanner data. *Int. J. Remote Sens.,* 9 (7), 1187-1200. http://dx.doi.org/10.1080/01431 168808 954928

Wulder, M.A., White, J.C., Goward, S.N., Masek, J.G., Irons, J.R., and Herold, M., et al. (2007). Landsat continuity: Issues and oppor -tuneties for land cover monitoring. *Remote Sens. Environ.,* 112 (3), 955-969. http://dx.doi.org/10.1016/j.rse.2007.07.004

Yool, S.R., Makaio, M.J., and Watts, J.M. (1997). Techniques for computer-assisted mapping of rangeland change. *J. Range Mana -ge.,* 50 (3), 307-314. http://dx.doi.org/10.2307/4003734

Yuan, D., Elvidge, C.D., and Lunetta, R.S. (1999). Survey of Multi-Spectral Methods for Land-Cover Change Analysis. In: Lu -netta, R.S., Elvidge, C.D. (Eds.), Remote sensing change detection: Environmental monitoring methods and applications. Taylor & Francis, London.

Zadeh, L. (1965). Fuzzy sets. *Inform. Control.,* 8 (3), 338-353. http://dx.doi.org/10.1016/S0019-9958(65)90241-X

Zadeh, L. (1984). Making computers think like people. *IEEE Spec -trum,* 26-32. http://dx.doi.org/10.1109/MSPEC.1984.6370431